Fabrication of nanoscale charge density wave systems

Katsuhiko Inagaki,[a] Takeshi Toshima, Satoshi Tanda, and Kazuhiko Yamaya
Department of Applied Physics, Graduate School of Engineering, Hokkaido University,
Kita 13 Nishi 8 Kita-ku, Sapporo 060-8628, Japan

Shinya Uji
National Institute for Materials Science, 1-2-1 Sengen, Tsukuba, Ibaraki 305-0047, Japan

Nanoscale charge density wave systems of quasi-one-dimensional o-TaS$_3$ crystals were fabricated. Gold electrodes 400 nm wide were made by standard lift-off technique on o-TaS$_3$ nanocrystals prepared by deposition on silicon substrates. Interface resistance was higher than 100 GΩ just after evaporation, and were significantly reduced by electron-beam irradiation. The electrodes were tested down to 80 mK, and were found quite durable for cryogenic measurement. The temperature dependence of the resistance of the nanocrystal was represented as the variable-range-hopping-type conduction with one dimension over the wide range of temperature, from 4.2 to 100 K. This behavior was different from that of conventional bulk samples. © *2005 American Institute of Physics.* [DOI: 10.1063/1.1862782]

The charge density wave (CDW) is an emergence of macroscopic quantum coherence of length greater than 1 μm, accompanied with lattice deformation of the wave vector $2k_F$.[1] Much attention has been given to nanoscale metal trichalcogenides (MX_3: M=Nb, Ta; X=Se, S) crystals due to their quasi-one-dimensional (1D) transport properties.[2–4] Reduction of the system size is expected to lead new macroscopic quantum phenomena because a whole nanocrystal becomes a single-domain CDW system, in contrast to a bulk crystal consisting of many CDW domains. Investigation of the nanoscale CDW system will be a key issue to realize prospecting applications, which exploit quantum collective motion of CDWs; for instance, field-effect transistors,[5] electron pumps,[6] and ultrafast memory.[7] Moreover, the recent discovery of MX_3 *topological* (ring, Möbius, and figure-of-eight) crystals[8] has opened a field of possible CDW devices by exploiting interference of long-range CDW order through their nontrivial topology. Since the system size must be smaller than the dephasing length of the CDW, the nanoscale CDW system is also crucial to observe the topological effect.

Studies on the nanoscale CDW were, however, often hindered by unexpectedly high interface resistance between the crystal and the electrodes.[2–5] To reduce interface resistance, various techniques were exploited; for example, fixing a sample to gold electrodes with glue,[2] and making use of soft metal (e.g., indium) as electrodes.[5] Therefore, a reproducible method for fabrication of electrodes is crucial for further study of the nanoscale MX_3 system. In additions, it is known that the electrodes themselves play an important role in the sliding dynamics of CDWs.[9] Hence, geometry of the electrodes should be determined rather than simply using rounded shapes of silver paint, which has been used to attach lead wires to samples.

We report here the fabrication of nanoscale CDW systems of o-TaS$_3$. The electrodes were fabricated by the standard electron-beam lithography technique. The contact resistance was too large to measure electrical properties, but it was found to be significantly improved after electron-beam irradiation. We found that the nanoscale o-TaS$_3$ crystal showed a variable-range-hopping (VRH) conduction over a wider range of temperatures than those observed in previous studies.

To obtain nanoscale o-TaS$_3$ samples, we synthesized single crystals by the chemical vapor transport method. A pure tantalum sheet and sulfur powder were put in a quartz tube. The quartz tube was evacuated to 1×10^{-6} Torr and heated in a furnace at 530 °C for 5 h. The reaction duration was chosen much shorter than the typical condition since we needed rather smaller crystals. The crystals were sonicated in toluene for 15 min and kept from perturbation for several hours to sediment unwanted larger crystals. The dispersion was then deposited on a silicon substrate with thermal oxide layer of 1 μm. After blow-drying, the crystals were inspected with an optical microscope. The obtained crystals were typically 0.2 μm in width and 10–100 μm in length.

Electrodes were fabricated by standard electron-beam lithography with a scanning electron microscope (SEM; JSM-5200, JEOL) equipped with a homemade writing system. On the substrate, 50-nm-thick gold markers and contact pads were written prior to deposition. Polymethylmethacrylate (PMMA) resist was spun to 500 nm thick, followed by prebaking at 170 °C for an hour. From the position of the crystal relative to the markers, a mask pattern was designed and loaded to the electron-beam writer. After the developing process by methyl isobutyl keton diluted by isopropylalcohol (1:2), 50-nm-thick gold thin film was evaporated. An adhesion layer of titanium was optionally evaporated between the gold and the substrate to investigate whether the adhesion layer affects the contact resistance. Lift-off was done with acetone at room temperature. We needed a further process to obtain an Ohmic contact. Each electrode was heated by irradiation of an electron beam with a SEM (JSM-820, JEOL). The electron current was monitored at the sample stage and by the probe current detector inserted in the beam line.

Figure 1 is a scanning electron micrograph of a TaS$_3$ crystal on a silicon substrate with gold electrodes. It is shown that the gold electrodes were well defined and located pre-
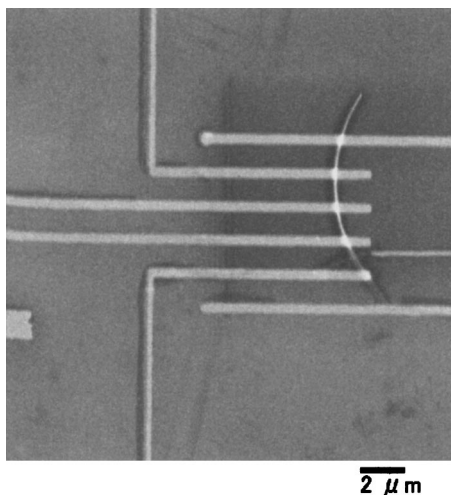
[a]Electronic mail: kina@eng.hokudai.ac.jp

2 μ m

FIG. 1. Scanning electron micrograph of an o-TaS$_3$ nanocrystal attached with gold electrodes.

cisely on the nanocrystal. The width of the electrode was 400 nm with a separation of 1 μm. Each electrode connects to a bonding pad (100×100 μm^2). We fabricated gold electrodes for several nanocrystals; however, roughly a half of them failed. In most cases of failure, the crystal was washed away at the lift-off stage. This was probably because of strong affinity between the TaS$_3$ surface and the PMMA. Another choice of electron beam resist rather than PMMA may solve the problem. The use of a Ti adhesive layer increased the yield on lift-off, although it affected contact resistance. We will discuss this problem shortly.

Figure 2(a) shows room-temperature I-V characteristics of the sample both before (the broken line) and after (the solid line) electron-beam treatment. The resistance was originally larger than 100 GΩ, while it decreased markedly to 21 kΩ after a 30 s irradiation of electron beam at an acceleration voltage of 25 kV and a beam current of typically 1 $\times 10^{-6}$ A. Since this was taken by two-terminal measurement, the obtained resistance consists of sample resistance, contact resistance, and the current-limiting series resistor of 2 kΩ. By taking into account the sample dimension $2 \times 0.2 \times 0.2$ μm^3, the resistivity is calculated as 3×10^{-4} Ω m. This
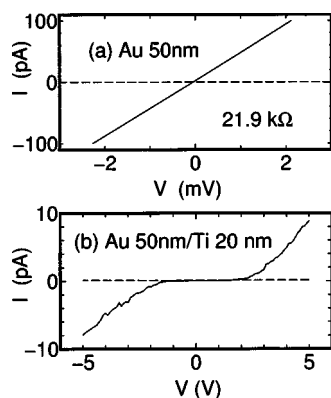

FIG. 2. I-V characteristics of TaS$_3$ nanocrystals with (a) 50-nm-thick gold electrodes only, and (b) 50-nm-thick gold electrodes with a 20-nm-thick Ti adhesive layer. The broken line and the solid line in each pane show the data before and after the electron-beam treatment, respectively. The solid curve in (a) shows that the Ohmic conduction of 21.9 kΩ is achieved for the electrodes without an adhesive layer. On the other hand, use of the Ti adhesive layers prevents Ohmic conduction (b).

is larger than the bulk resistivity by two orders. The cross section that actually effects electric conduction is 10^{-2} of that which appears in the micrograph, if the resistivity is same as the bulk sample. Previous studies of o-TaS$_3$ thin wires have shown a similar tendency.[3]

Ohmic conduction was not obtained for the electrode with a Ti adhesive layer. Figure 2(b) shows the I-V curves of before (the broken line) and after (the solid line) the electron irradiation. The curve did not change after the electron beam was irradiated for a period longer than 30 s. Titanium is chemically active and easily forms a bond to other materials. That is why it is often used as an adhesive layer between the substrate and the electrode. From the obtained I-V curves, we believe a thin Ti layer was oxidized or sulfurized when it was deposited onto the o-TaS$_3$ surface, and it became a tunnel barrier.

During irradiation of an electron beam in SEM, the sample sometimes gets dirty due to contamination with carbonate. We believe this plays a small role in the transport measurements for the following reasons. (1) The typical sample size is 10–100 μm in length, and we use the optical microscope for locating of the sample. (2) Since the gold electrodes are evaporated after deposition of the sample, the metal layer covers and protects the contact area during irradiation. (3) The electron beam is irradiated only on the metal-sample contact, which is to be heated locally, although a weak electron beam is scattered when we look at the sample. The difference between the I-V characteristics shown in Figs. 2(a) and 2(b) supports our observation.

The fabricated electrodes were found to be very durable. We cooled the electrodes to 80 mK several times, and observed no degrading of the electrode. Even after storage for six months, electric properties showed only little change. This is very astonishing because conventional methods to attach the electrodes on MX_3 crystals are fragile and can only be used for a couple of measurements. Hence, our method will be important for future applications of MX_3 nanocrystals to electronics.

Let us discuss the temperature dependence of resistance of the nanoscale o-TaS$_3$ crystal. It is known that the temperature dependence of the resistance of conventional bulk samples is complex and consists of several regimes. At room temperature, a bulk o-TaS$_3$ crystal is metallic. Below the Peierls temperature ($T_P \sim 220$ K), the resistance rises exponentially [$\exp(\Delta/k_B T)$], where $\Delta \sim 800$ K. At lower temperatures than ~ 100 K, the potential of exponential rise changes $\Delta \sim 200$ K. This change in the potential is described in terms of "soliton transport".[10] Below 20 K, the formula of the temperature dependence changes from the Arrhenius form to VRH conduction, represented as

$$\sigma(T) = \sigma_0 \exp[-(T_0/T)^{1/(d+1)}], \tag{1}$$

where T_0 is a characteristic temperature and $d=1$ is dimension of the system.[11,12]

On the other hand, the observed temperature dependence of the nanoscale o-TaS$_3$ crystal was significantly different from that of the bulk crystals. Figure 3 shows the o-TaS$_3$ nanocrystal differs from that of the bulk samples at the following points: (1) Peierls transition was not clearly observed in the nanocrystal, and (2) resistance was described in terms of VRH conduction over the wide range of temperatures (100 to 4.2 K) with $d=1$ (inset of Fig. 3).
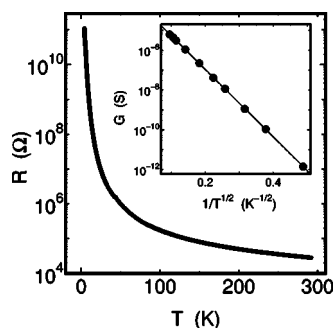
FIG. 3. Temperature dependence of resistance of the o-TaS$_3$ nanocrystal. Inset shows the linear conductance from 4.2 to 100 K as a function of $T^{-1/2}$. The data fit to a linear line very well, suggesting VRH conduction: $\sigma \propto \exp[-(T_0/T)^{1/2}]$.

The first feature is interpreted as the result of 1D fluctuation because the cross section is small enough.[3] The CDW actually occurs in "quasi"-1D materials, consisting of a bundle of conductive chains. The CDW phase is stabilized by correlating adjacent chains through a Coulomb interaction. If the cross section, and hence the number of the chains, is reduced, the system cannot gain its free energy by the mechanism of Peierls transition. We believe that the interpretation is consistent with our sample whose cross section is 4×10^{-2} μm^2.

Another feature is rather surprising. The observed resistance fell into the VRH relation (1) with good agreement over the wide range of temperatures. The physical picture of the VRH conduction is, however, inconsistent with the standard CDW mechanism. Assumptions for deriving Eq. (1) include a finite density of states at the Fermi level.[13] In the CDW state of o-TaS$_3$, the whole Fermi surface is relevant to the transition and no electron density remains.[14] That is why previous studies for bulk crystals showed good agreement in the Arrhenius form.

Actually, the previous studies of o-TaS$_3$ were unlikely to provide acceptable interpretation of the VRH conduction, although it must be related with randomly distributed impurities. We believe that in this regime the carrier is dislocation of the CDW, or charged soliton. The energy to excite a soliton differs in each position due to impurities. Further studies will unveil the physical nature of the VRH conduction in o-TaS$_3$ by careful comparison of nanoscale samples with conventional bulk ones.

[1] G. Grüner, *Density Waves in Solids* (Addison-Wesley Longman, Reading, MA, 1994).

[2] H. S. J. van der Zant, E. Slot, S. V. Zaitsev-Zotov, and S. N. Artemenko, Phys. Rev. Lett. **87**, 126401 (2001).

[3] S. V. Zaïtsev-Zotov, V. Ya. Pokrovskiĭ, and P. Monceau, JETP Lett. **73**, 25 (2001).

[4] D. V. Borodin, S. V. Zaïtsev-Zotov, and F. Ya. Nad', Sov. Phys. JETP **63**, 184 (1986).

[5] T. L. Adelman, S. V. Zaitsev-Zotov, and R. E. Thorne, Phys. Rev. Lett. **74**, 5264 (1995).

[6] M. I. Visscher and G. E. W. Bauer, Appl. Phys. Lett. **75**, 1007 (2002).

[7] D. Mihailović, D. Dvorsek, V. V. Kabanov, J. Demsar, L. Forro, and H. Berger, Appl. Phys. Lett. **80**, 871 (2002).

[8] S. Tanda, T. Tsuneta, Y. Okajima, K. Inagaki, K. Yamaya, and N. Hatakenaka, Nature (London) **417**, 397 (2002).

[9] N. P. Ong, G. Verma, and K. Maki, Phys. Rev. Lett. **52**, 663 (1984).

[10] T. Takoshima, M. Ido, K. Tsutsumi, T. Sambongi, S. Honma, K. Yamaya, and Y. Abe, Solid State Commun. **35**, 911 (1980).

[11] S. K. Zhilinskiĭ, M. E. Itkis, I. Yu. Kal'nova, F. Ya. Nad', and V. B. Preobrazhenskiĭ, Sov. Phys. JETP **58**, 211 (1983).

[12] M. E. Itkis, F. Ya. Nad', and P. Monceau, J. Phys.: Condens. Matter **2**, 8327 (1990).

[13] N. F. Mott, *Metal-Insulator Transition*, 2nd ed. (Taylor & Francis, London, 1990).

[14] This is contrast to the case of NbSe$_3$, in which not all of the Fermi surface contributes to the Peierls transition, and there still remain electron states even after the transition.